# Effects of low-viscosity post-perovskite on thermo-chemical mantle convection in a 3-D spherical shell

Takashi Nakagawa[1] and Paul J. Tackley[1]

[1] Numerical simulations of thermo-chemical, multi-phase mantle convection in a 3-D spherical shell are performed to determine how a low viscosity of post-perovskite affects dynamics and structures in the deep mantle. Low-viscosity post-perovskite weakens the deepest part of slabs, allowing them to more effectively spread over the core-mantle boundary (CMB), and it also results in a greater volume of basalt segregating, both of which increase the size of dense chemical piles, the horizontal lengthscale of regions of pooled slab material, and the steepness of piles' edges (in composition and phase), consistent with the existence of steep, sharp-sided edges found in seismic analyses. CMB heat flux is strongly enhanced in regions of low-viscosity post-perovskite (consistent with a theoretical prediction) and both CMB and surface heat flux are increased on average by a low-viscosity of post-perovskite, which could have important implications for the evolution of Earth's core and mantle. **Citation:** Nakagawa, T., and P. J. Tackley (2011), Effects of low-viscosity post-perovskite on thermo-chemical mantle convection in a 3-D spherical shell, *Geophys. Res. Lett.*, *38*, L04309, doi:10.1029/2010GL046494.

## 1. Introduction

[2] Post-perovskite is now established as an important phase in the deepest mantle. High pressure experiments [*Hunt et al.*, 2009; *Yamazaki et al.*, 2006; *Yoshino and Yamazaki*, 2007] and first principle calculations of atomic diffusion [*Ammann et al.*, 2010] indicate that the viscosity of post-perovskite is lower than that of perovskite- by a factor of $O(10^3)$ to $O(10^4)$ according to [*Ammann et al.*, 2010]. Geodynamical instantaneous flow modeling has shown that the long-wavelength geoid is very sensitive to the presence of low viscosity post-perovskite regions at the base of cold subducted slabs reaching the CMB [*Tosi et al.*, 2009; *Ghosh et al.*, 2010]. Thus, it is important to determine the influence of low post-perovskite viscosity in long-term dynamical calculations.

[3] Dynamical calculations should also include compositional variations, because compositional anomalies (in the form of dense 'piles') are widely thought to exist above the core-mantle boundary (CMB) in order explain seismological observations [*Trampert et al.*, 2004; *Ni et al.*, 2002; *To et al.*, 2005], often in combination with post-perovskite [*Lay et al.*, 2006; *van der Hilst et al.*, 2007]. Such compositional anomalies also have a strong influence on CMB topography [*Lassak et al.*, 2007, 2010; *Yoshida*, 2008], although these studies did not consider post-perovskite.

[4] Other geodynamically important quantities are the heat flux across the CMB and its lateral variation, both of which have a first-order influence on the geodynamo and the evolution of the core, and which are influenced by compositional anomalies and post-perovskite [*Nakagawa and Tackley*, 2008, 2010]. Heat transfer by mantle convection across the CMB may well be different when the post-perovskite has a lower viscosity than perovskite, as predicted by a theoretical investigation [*Buffett*, 2007] and a two-dimensional isochemical study [*Cizkova et al.*, 2010].

[5] Thus, in this study, the dynamical influences of weak post-perovskite are investigated using numerical thermo-chemical mantle convection simulations in a 3-D spherical shell, focusing on various diagnostics related to structures and dynamics in the CMB region.

## 2. Model Description

[6] The physical model and numerical solution method are very similar to those in our previous papers [e.g., *Nakagawa and Tackley*, 2005a, 2005b, 2006, 2010]), so only an overview and pertinent differences are given here. Compressibility is included using the truncated anelastic approximation, and the equations are solved in a 3-D spherical shell using the code StagYY [*Tackley*, 2008]. Two systems of phase transitions, those in the olivine and pyroxene-garnet systems, are included, as listed in Table 2. The density difference at the CMB is 3.6%, which corresponds to 2.16% between MORB and pyrolite. The mantle is assumed to be a mechanical mixture of basalt and harzburgite, starting with uniform pyrolite (20% basalt) [*Xu et al.*, 2008], then compositional anomalies are generated by melt-induced differentiation producing oceanic crust.

[7] Isothermal boundary conditions are applied at both top and bottom boundaries, which are set at 300 K and 4173 K, respectively. Here the CMB temperature is fixed: core cooling is not taken into account. With the assumed CMB temperature and post-perovskite phase change parameters, a double-crossing of the perovskite to postperovskite transition [*Hernlund et al.*, 2005] is expected.

[8] The viscosity law assumes linear diffusion creep, because [*Ammann et al.*, 2010] find a diffusion creep viscosity that is $O(10^3)$ lower than that for perovskite [*Ammann et al.*, 2009]. It is possible that post-perovskite deforms mainly by dislocation creep (as assumed in some previous studies [*Cizkova et al.*, 2010; *van den Berg et al.*, 2010]), which would further lower the viscosity. The viscosity law

---

[1]Institute of Geophysics, ETH Zurich, Zurich, Switzerland.

**Table 1.** Mantle Model Physical Parameters[a]

| Symbol | Meaning | Non-D. Value | Dimensional Value |
|---|---|---|---|
| $Ra_0$ | Reference Rayleigh number | $10^7$ | N/A |
| $\eta_0$ | Reference viscosity | 1 | $1.4 \times 10^{22}$ Pa s |
| $\Delta\eta_{pv}$ | Viscosity jump at 660 km | 30 | N/A |
| $\Delta\eta_{ppv}$ | Viscosity jump at the post-perovskite boundary | 1 or 0.001 | N/A |
| $\sigma_b$ | Yield stress at surface | $8.5 \times 10^4$ | 100 MPa |
| $\sigma_d$ | Yield stress gradient | $3.4 \times 10^5$ | 138.0 Pa m$^{-1}$ |
| $\rho_0$ | Reference (surface) density | 1 | 3300 kg m$^{-3}$ |
| g | Gravity | 1 | 9.8 m s$^{-2}$ |
| $\alpha_0$ | Ref. (surface) thermal expan. | 1 | $5 \times 10^{-5}$ K$^{-1}$ |
| $\kappa_0$ | Ref. (surface) thermal diff. | 1 | $7 \times 10^{-7}$ m$^2$ s$^{-1}$ |
| $\Delta T_{sa}$ | Temperature scale | 1 | 2500 K |
| H | Internal heating rate at the present time | 13.8 | $3.7 \times 10^{-12}$ W/kg |

[a]$Ra_0 = \rho_0 g \alpha_0 \Delta T_{sa} d^3 / \kappa_0 \eta_0$.

is as by *Keller and Tackley* [2009] with the addition of plastic yielding to produce plate-like behavior:

$$\eta_d(T,z) = A_0 \left[ \prod_{ij} \Delta\eta_{ij}\Gamma_{ij}f_j \right] \exp\left[ \frac{13.801 + 11.22d}{T} \right]$$

$$\eta_Y = \frac{\sigma_0 + \sigma_1 z}{2\dot{e}} \qquad (1)$$

$$\eta = \left( \frac{1}{\eta_d} + \frac{1}{\eta_Y} \right)^{-1}$$

where T is absolute nondimensional temperature, d is nondimensional depth, $\Delta\eta_{ij}$ is the viscosity jump due to each phase transition, $\Gamma_{ij}$ is the phase function for phase $i$ in system $j$ (varying from 0 at low pressure to 1 at high pressure) and f$_j$ is the fraction of phase system $j$ present. $A_0$ is a constant calculated such that the viscosity is equal to 1 at $T = 1600$ K and zero depth, $\sigma_0$ and $\sigma_1$ are yield stress at zero depth and yield stress gradient respectively, and $\dot{e}$ is the second invariant of the strain rate tensor. The activation energy and volume are based on those of perovskite [*Yamazaki and Karato*, 2001].

[9] Physical parameters used here are listed in Table 1 and phase transition parameters are listed in Table 2.

[10] The initial condition is an adiabatic temperature plus thin thermal boundary layers at the top and bottom, plus small random perturbations. The numerical resolution is $64 \times 192 \times 64 \times 2$ with 20 million tracers to track chemical composition and melt fraction.

## 3. Results

[11] Here two cases are examined: one with post-perovskite having the same viscosity as perovskite, and one with low-viscosity post-perovskite. Figure 1 shows the heat flux across the surface and CMB as a function of time. With low-viscosity post-perovskite the heat flux across the CMB displays a huge time variation and is generally higher than with regular post-perovskite, consistent with findings from 2-D isochemical simulations [*Cizkova et al.*, 2010]. The surface heat flow is much less time-dependent, and is also slightly higher with low-viscosity post-perovskite. It indicates that the system has reached statistically steady state.

[12] Figure 2 shows thermo-chemical-phase structures for regular and weak post-perovskite cases after 4.5 Gyrs of evolution. Cold slab-like downwellings penetrate to the CMB region, where they are transformed to post-perovskite, and push dense segregated basalt aside to form piles. Low

post-perovskite viscosity amplifies this effect because it enables slabs to more easily deform and spread over the CMB. Additionally, in the weak post-perovskite case there is a ~50% greater volume of segregated basalt due to some combination of more efficient separation of basalt from the slab and faster processing arising from higher velocities. For both of these reasons, 'piles' in the weak-pPv case are thicker and have a larger length-scale than those in the standard case. This indicates that it is density differences that are responsible for maintaining piles, not mechanical strength. An anticorrelation between the locations of dense material and post-perovskite is observed, as was previously found in similar cases in 2-D cylindrical [*Nakagawa and Tackley*, 2005a, 2005b] and 3-D Cartesian geometries [*Nakagawa and Tackley*, 2006]. Both the piles and post-perovskite regions have sharp edges, which tend to be more pronounced with low-viscosity post-perovskite.

[13] Figure 3 shows CMB topography, CMB heat flux, and temperature and composition at 2790 km depth. The amplitude of CMB topography ranges from approximately −5 km to 5 km with regular post-perovskite, being strongly negative (depressed) under slabs, positive around the edges of slabs, and neutral under 'piles', consistent with previous results [*Lassak et al.*, 2007, 2010]. This range is larger than in some previous numerical mantle convection simulations [*Lassak et al.*, 2010] and an instantaneous flow model [*Yoshida*, 2008]. When low-viscosity post-perovskite is included the amplitude of topography is greatly reduced, ranging from around −2 km to 2 km, the main difference being that topography is no longer strongly negative under

**Table 2.** Physical Parameters for Two-Component Phase Changes Modified From *Tackley and Xie* [2003] to Include the Post-Perovskite Phase Transition[a]

| # | Depth (km) | Temperature (K) | $\Delta\rho_{ph}$ (kg m$^{-3}$) | $\gamma$ (MPa/K) | Width (km) |
|---|---|---|---|---|---|
| | *Olivine-Spinel-Perovskite-Postperovskite* | | | | |
| 1 | 410 | 1600 | 280 | +2.5 | 30.0 |
| 2 | 660 | 1900 | 400 | −2.5 | 30.0 |
| 3 | 2740 | 2650 | 60 | +12.0 | 30.0 |
| | *Pyroxene-Garnet-Perovskite-Postperovskite* | | | | |
| 1 | 60 | 0 | 350 | 0 | 30.0 |
| 2 | 400 | 1600 | 100 | +1.0 | 75.0 |
| 3 | 720 | 1900 | 500 | +1.0 | 75.0 |
| 4 | 2700 | 2650 | 60 | +12.0 | 30.0 |

[a]The 60 km deep phase change in the pyroxene-garnet-perovskite system corresponds to the basalt-eclogite transition.
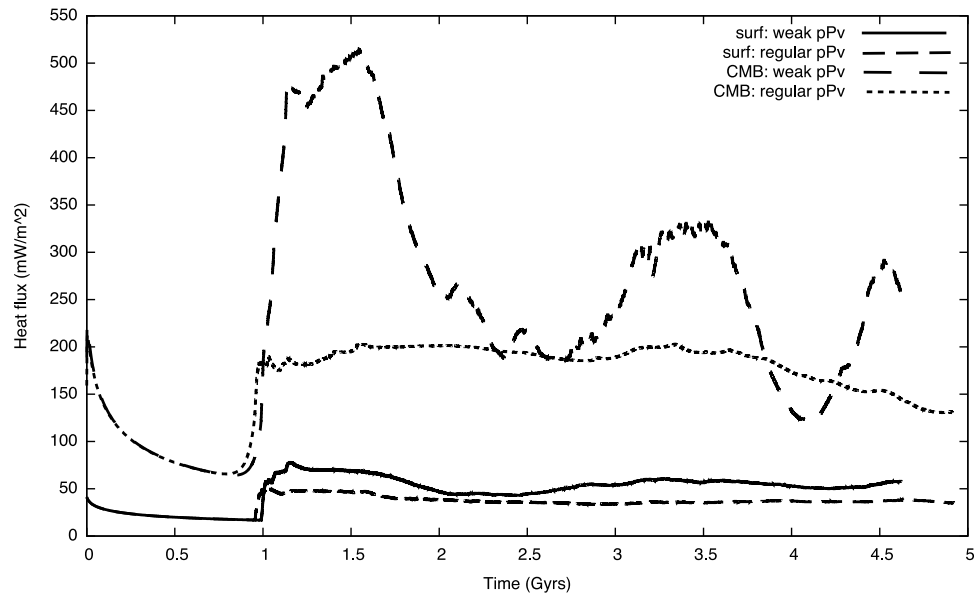
**Figure 1.** Surface and CMB heat flux as a function of time.

slabs, because their low viscosity in the CMB region reduces the coupling to higher-up part of slabs and allows them to spread more. CMB heat flux is high where cold slab material pools above the CMB, which occurs in broader regions when post-perovskite viscosity is low, thereby enhancing the total CMB heat flux. Additionally, the max-

imum CMB heat flux is higher with low-viscosity post-perovskite. This observed enhancement of CMB heat flux was previously predicted from a theoretical estimate between the velocity of subduction, the viscosity in the CMB region and CMB heat flux [*Buffett*, 2007]. In general,
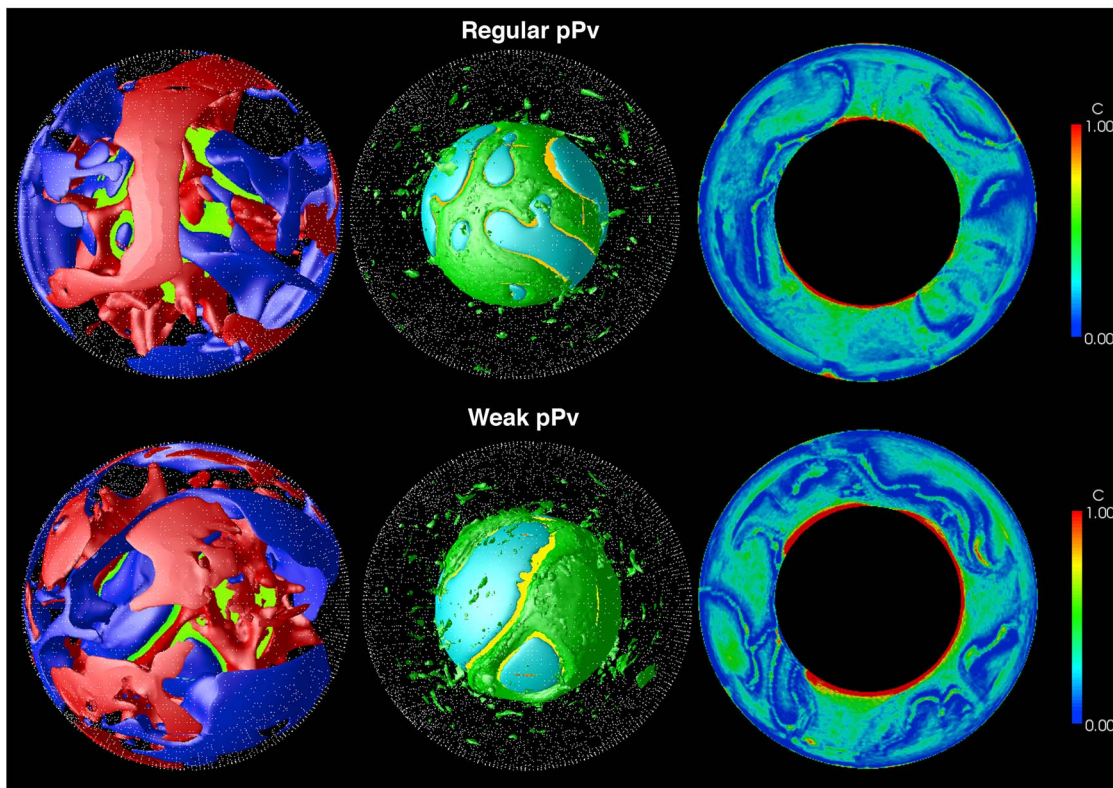


**Figure 2.** The thermo-chemical-phase state after 4.5 Ga of evolution. (top) With regular post-perovskite. (bottom) With low-viscosity post-perovskite. (left) Isosurfaces of residual temperature (red: +250 K; blue: −250 K compared to geotherm). (right) Isosurfaces of composition (green: 75% basalt) and post-perovskite (cyan).
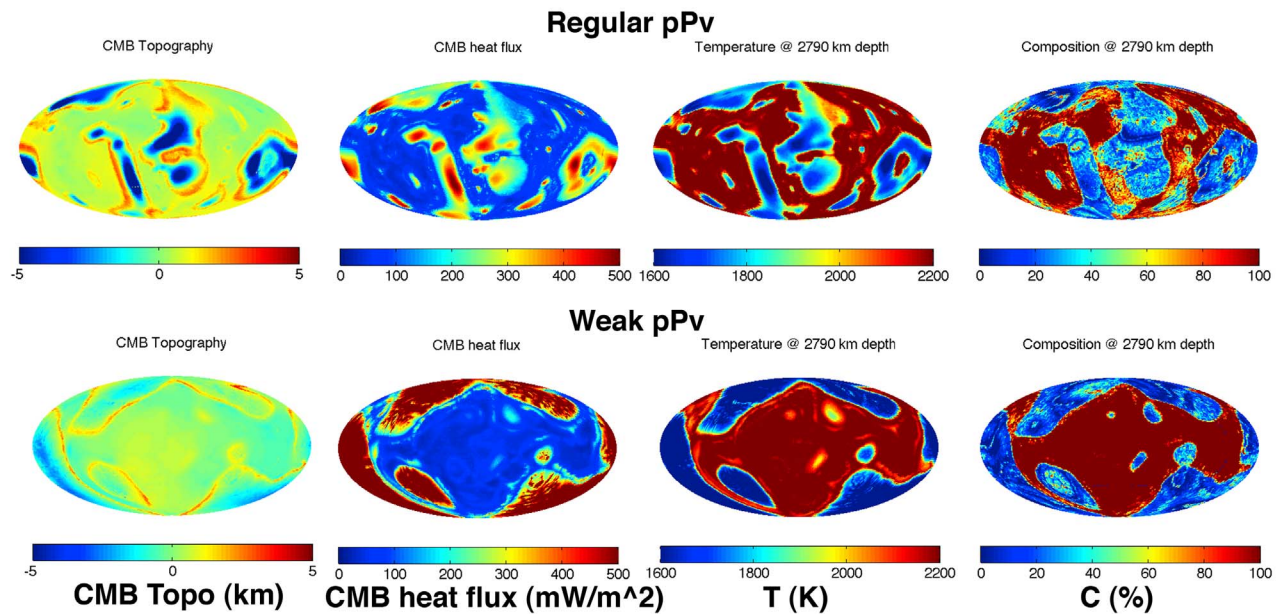
**Figure 3.** CMB topography and heat flux, and temperature and composition at 2790 km depth (100 km above the CMB) (from left to right, respectively for the same cases and time as Figure 3. (top) Regular post-perovskite. (bottom) Low-viscosity post-perovskite.

a low post-perovskite viscosity appears to suppress small-scale structures.

[14] Figure 4 shows the viscosity at 2790 km depth, where the post-perovskite phase transition is found. Comparing this to the temperature distribution shown in Figure 3, a viscosity reduction in cold pooled slab regions is clearly visible. This causes the reduced CMB topography and enhancement of CMB heat flux discussed above.

## 4. Summary and Discussion

[15] Here we have investigated the effect of low-viscosity post-perovskite in the CMB region on thermo-chemical mantle convection. The major findings are as follows.

[16] 1. Low post-perovskite viscosity amplifies the size of dense compositional piles above the CMB, because it enables cold slab material to spread more easily above the CMB, pushing dense segregated basalt aside into piles, and also because a larger volume of basalt segregates at the CMB when the post-perovskite viscosity is low. It is plausible, although not studied here, that this greater segregated basalt volume is because low viscosity facilitates more efficient segregation of the basaltic and harzburgitic parts of the slab. As a result, structures in the CMB region tend to be of longer wavelength when low-viscosity post-perovskite is present. Steep, sharp-sided edges of both post-perovskite regions and dense piles are enhanced by the effects of low-viscosity post-perovskite, consistent with seismic waveform analyses suggesting the existence of steep, sharp-sided edges between slow and fast anomalies [*Ni et al.*, 2002; *To et al.*, 2005]. We find steep, sharp edges even when the dense material has an identical compressibility, contrary to *Tan and Gurnis* [2005], which is something that could be further tested in the future.

[17] 2. CMB topography is reduced by the presence of low-viscosity post-perovskite. With regular-viscosity post-

perovskite, the CMB is depressed where slabs arrive and neutral elsewhere [*Lassak et al.*, 2010], resulting in a strong correlation between CMB topography and temperature above the CMB. With low-viscosity post-perovskite, slab pools are weak and broad and do not depress the CMB, which removes most of this correlation. Thus the correlation (or lack of it) between temperature above the CMB and CMB topography inferred from seismic waveform analyses [*Tanaka*, 2010] could be used as a diagnostic to test for the viscosity of post-perovskite. A previous instantaneous mantle flow model [*Yoshida*, 2008] pointed out the effect of
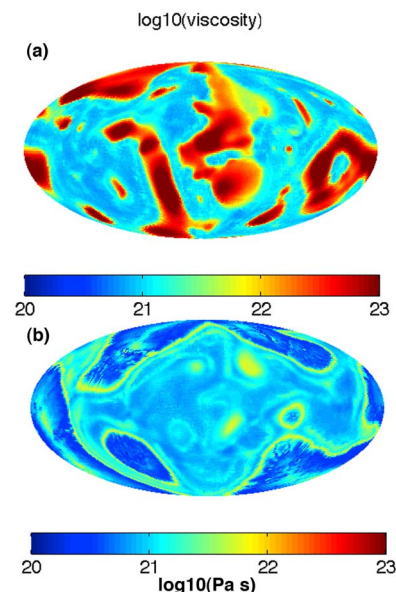
**Figure 4.** Viscosity at 2790 km depth (100 km above the CMB). (a) Regular post-perovskite. (b) Weak post-perovskite.

a low-viscosity D″ in reducing CMB topography but there, low-viscosity was imposed everywhere above the CMB, whereas here it is due low-viscosity post-perovskite in cold regions and temperature-dependent viscosity in hot regions (containing piles).

[18] 3. Low-viscosity post-perovskite substantially increases heat transfer across the CMB by increasing the pooling of cold slab material above the CMB. This is consistent with a theoretical prediction between the viscosity of post-perovskite and CMB heat flux [*Buffett*, 2007], and iso-chemical 2-D calculations [*Cizkova et al.*, 2010]. As a result it also slightly increases heat flux across the surface. This would have a significant effect on core cooling and hence the thermal evolution of the mantle and core, which are not studied here for the purpose of simplicity.

[19] There are several other interesting effects of low viscosity post-perovskite that we plan to study in future. The effect on geoid found in instantaneous flow models [*Tosi et al.*, 2009; *Ghosh et al.*, 2010] should be tested in full convection models. The pattern of anisotropy in the deep mantle, an important seismological observation [e.g., *Wookey et al.*, 2005], is expected to be strongly influenced both by strongly anisotropic post-perovskite seismic velocity and by the change in flow patterns caused by low post-perovskite viscosity. The dependence of results on uncertain parameters such as the density difference between basalt and harzburgite in the deep mantle and exact viscosity reduction, should be systematically evaluated.

## References

Ammann, M. W., J. P. Brodholt, and D. P. Dobson (2009), DFT study of migration enthalpies in MgSiO$_3$ perovskite, *Phys. Chem. Miner.*, *36*, 151–158, doi:10.1007/s00269-008-0265-z.

Ammann, M. W., J. P. Brodholt, J. Wookey, and D. P. Dobson (2010), First-principles constraints on diffusion in lower-mantle minerals and a weak D″ layer, *Nature*, *465*, 462–465, doi:10.1038/nature09052.

Buffett, B. A. (2007), A bound on heat flow below a double crossing of the perovskite-postperovskite phase transition, *Geophys. Res. Lett.*, *34*, L17302, doi:10.1029/2007GL030930.

Cizkova, H., O. Cadek, C. Matyska, and D. A. Yuen (2010), Implications of post-perovskite properties for core-mantle dynamics, *Phys. Earth Planet. Inter.*, *180*, 235–243, doi:10.1016/j.pepi.2009.08.008.

Ghosh, A., T. W. Becker, and S. J. Zhong (2010), Effects of lateral viscosity variations on the geoid, *Geophys. Res. Lett.*, *37*, L01301, doi:10.1029/2009GL040426.

Hernlund, J., C. Thomas, and P. J. Tackley (2005), Phase boundary double-crossing and partial melting in Earth's deepest mantle, *Nature*, *434*, 882–886, doi:10.1038/nature03472.

Hunt, S. A., D. J. Weidner, L. Li, L. Wang, N. P. Walte, J. P. Brodholt, and D. P. Dobson (2009), Weakening of calcium iridate during its transformation from perovskite to post-perovskite, *Nat. Geosci.*, *2*, 794–797, doi:10.1038/ngeo663.

Keller, T., and P. J. Tackley (2009), Towards self-consistent modeling of the Martian dichotomy: The influence of low-degree convection on crustal thickness distribution, *Icarus*, *202*, 429–443, doi:10.1016/j.icarus.2009.03.029.

Lassak, T. M., A. K. McNamara, and S. Zhong (2007), Influence of thermochemical piles on topography at Earth's core-mantle boundary, *Earth Planet. Sci. Lett.*, *261*, 443–455, doi:10.1016/j.epsl.2007.07.015.

Lassak, T. M., A. K. McNamara, E. J. Garnero, and S. Zhong (2010), Core-mantle boundary topography as a possible constraint on lower mantle chemistry and dynamics, *Earth Planet. Sci. Lett.*, *289*, 232–241, doi:10.1016/j.epsl.2009.11.012.

Lay, T., J. Hernlund, E. J. Garnero, and M. S. Thorne (2006), A post-perovskite lens and D″ heat flux beneath the central Pacific, *Science*, *314*, 1272–1276, doi:10.1126/science.1133280.

Nakagawa, T., and P. J. Tackley (2004), Effects of perovskite-post perovskite phase change near core-mantle boundary in compressible mantle convection, *Geophys. Res. Lett.*, *31*, L16611, doi:10.1029/2004GL020648.

Nakagawa, T., and P. J. Tackley (2005a), The interaction between the post-perovskite phase change and a thermo-chemical boundary layer near the core-mantle boundary, *Earth Planet. Sci. Lett.*, *238*, 204–216, doi:10.1016/j.epsl.2005.06.048.

Nakagawa, T., and P. J. Tackley (2005b), Deep mantle heat flow and thermal evolution of the Earth's core based on thermo-chemical multiphase mantle convection, *Geochem. Geophys. Geosyst.*, *6*, Q08003, doi:10.1029/2005GC000967.

Nakagawa, T., and P. J. Tackley (2006), Three-dimensional structures and dynamics in the deep mantle: Effects of post-perovskite phase change and deep mantle layering, *Geophys. Res. Lett.*, *33*, L12S11, doi:10.1029/2006GL025719.

Nakagawa, T., and P. J. Tackley (2008), Lateral variations in CMB heat flux and deep mantle seismic velocity caused by thermal-chemical-phase boundary layer in 3D spherical convection, *Earth Planet. Sci. Lett.*, *271*, 348–358, doi:10.1016/j.epsl.2008.04.013.

Nakagawa, T., and P. J. Tackley (2010), Influence of initial CMB temperature and other parameters on the thermal evolution of Earth's core resulting from thermochemical spherical mantle convection, *Geochem. Geophys. Geosyst.*, *11*, Q06001, doi:10.1029/2010GC003031.

Ni, S., E. Tan, M. Gurnis, and D. V. Helmberger (2002), Sharp sides to the African superplume, *Science*, *296*, 1850–1852, doi:10.1126/science.1070698.

Tackley, P. J. (2008), Modelling compressible mantle convection with large viscosity contrasts in a three-dimensional spherical shell using yin-yang grid, *Phys. Earth Planet. Inter.*, *171*, 7–18, doi:10.1016/j.pepi.2008.08.005.

Tackley, P. J., and S. Xie (2003), Stag3D: A code for modeling thermo-chemical multiphase convection in Earth's mantle, in *Computational Fluid and Solid Mechanics 2003: Proceedings, Second MIT Conference on Computational Fluid and Solid Mechanics, June 17–20, 2003*, edited by K. J. Bathe, pp. 1524–1527, Elsevier, Amsterdam.

Tan, E., and M. Gurnis (2005), Metastable superplumes and mantle compressibility, *Geophys. Res. Lett.*, *32*, L20307, doi:10.1029/2005GL024190.

Tanaka, S. (2010), Constraints on the core-mantle boundary topography from P4KP-PcP differential travel times, *J. Geophys. Res.*, *115*, B04310, doi:10.1029/2009JB006563.

To, A., B. Romanowicz, Y. Capdeville, and N. Takeuchi (2005), 3D effects of sharp boundaries at the borders of the African and Pacific super-plumes, *Earth Planet. Sci. Lett.*, *233*, 137–153, doi:10.1016/j.epsl.2005.01.037.

Tosi, N., O. Cadek, Z. Martinec, D. A. Yuen, and G. Kaufmann (2009), Is the long-wavelength geoid sensitive to the presence of postperovskite above the core-mantle boundary?, *Geophys. Res. Lett.*, *36*, L05303, doi:10.1029/2008GL036902.

Trampert, J., F. Deschamps, J. Resovsky, and D. Yuen (2004), Probabilistic tomography maps significant chemical heterogeneities in the lower mantle, *Science*, *306*, 853–856, doi:10.1126/science.1101996.

van den Berg, A. P., M. V. De Hoop, D. A. Yuen, A. Duchkov, R. D. van der Hilst, and M. H. G. Jacobs (2010), Geodynamical modeling and multiscale seismic expression of thermo-chemical heterogeneity and phase transitions in the lowermost mantle, *Phys. Earth Planet. Inter.*, *180*, 244–257, doi:10.1016/j.pepi.2010.02.008.

van der Hilst, R. D., W. V. de Hoop, P. Wang, S.-H. Shim, P. Ma, and L. Tenorio (2007), Seismostratigraphy and thermal structure of Earth's core-mantle boundary region, *Science*, *315*, 1813–1817, doi:10.1126/science.1137867.

Wookey, J., S. Stackhouse, J. M. Kendall, J. Brodholt, and G. D. Price (2005), Efficacy of the post-perovskite phase as an explanation for lowermost-mantle seismic properties, *Nature*, *438*, 1004–1007, doi:10.1038/nature04345.

Xu, W. B., C. Lithgow-Bertelloni, L. Stixrude, and J. Ritsema (2008), The effect of bulk composition and temperature on mantle seismic structure, *Earth Planet. Sci. Lett.*, *275*, 70–79, doi:10.1016/j.epsl.2008.08.012.

Yamazaki, D., and S.-I. Karato (2001), Some mineral physics constraints on the rheology and geothermal structure of Earth's lower mantle, *Am. Mineral.*, *86*, 385–391.

Yamazaki, D., T. Yoshino, H. Ohfuji, J. Ando, and A. Yonea (2006), Origin of seismic anisotropy in the D″ layer inferred from shear deformation experiments on post-perovskite phase, *Earth Planet. Sci. Lett.*, *252*, 372–378, doi:10.1016/j.epsl.2006.10.004.

Yoshida, M. (2008), Core-mantle boundary topography estimated from numerical simulations of instantaneous flow, *Geochem. Geophys. Geosyst.*, *9*, Q07002, doi:10.1029/2008GC002008.

Yoshino, T., and D. Yamazaki (2007), Grain growth kinetics of CaIrO$_3$ perovskite and post-perovskite with implications for rheology of D″ layer, *Earth Planet. Sci. Lett.*, *255*, 485–493, doi:10.1016/j.epsl.2007. 01.010.

Zhang, S., and U. Christensen (1993), Some effects of lateral viscosity variations on geoid and surface velocity induced by density anomalies in the mantle, *Geophys. J. Int.*, *114*, 531–547, doi:10.1111/j.1365-246X.1993.tb06985.x.

Zhong, S., A. K. McNamara, E. Tan, L. Moresi, and M. Gurnis (2008), A benchmark study on mantle convection in a 3-D spherical shell using CitcomS, *Geochem. Geophys. Geosyst.*, *9*, Q10017, doi:10.1029/ 2008GC002048.

T. Nakagawa and P. J. Tackley, Institute of Geophysics, ETH Zurich, Sonneggstrasse 5, CH-8092 Zurich, Switzerland. (ntakashi@ethz.ch)